Gas Phase Reaction of Neutral Carbon Disulfide with Its Hydride Adduct Anions: Tandem Mass Spectrometry and Theoretical Studies

Y. Gimbert* and R. Arnaud

Université Joseph Fourier, LEDSS, BP 53X, 38041 Grenoble Cedex, France

J.-C. Tabet

Université Pierre et Marie Curie, Paris VI, Laboratoire de Chimie Organique Structurale, 75230 Paris, France

Ed. de Hoffmann

Université Catholique de Louvain, Laboratoire de Spectromètrie de Masse, 1348 Louvain la Neuve, Belgium

Received: September 22, 1997; In Final Form: March 3, 1998

In a chemical ionization source with CH_4/N_2O, carbon disulfide (CS_2) yields its radical anion by electron capture and CHS_2^- by hydride attachment. By combining tandem mass spectrometric experiments and theoretical ab initio calculations, we demonstrate that hydride attachment can yield either thioformate anion or thiohydroxythiocarbonyl carbanion without interconversion. The thioformate anion reacts with neutral at CS_2 carbon, whereas the syn thiohydroxythiocarbonyl carbanion attacks at the sulfur site to ultimately form $HSCS_2^-$ and CS species.

Introduction

Studies on the formation, and reactions of gas-phase anions have provided useful methods for elucidating carbanion structure and reaction mechanisms.[1] The gas-phase chemistry of anion−molecule reaction of organo−sulfur has been extensively investigated by a large variety of experimental methods.[2] The experimental determination of isomeric ion structures in the gas phase is a difficult task. Collision-induced dissociation (CID) is a well-known method for investigating the structures of ions.[3] Another application of CID is for the generation of anions that cannot be obtained easily by other means. However, whether the anions are generated by CID or ion−molecule reactions, in most cases additional experiments are required to determine their structure. For this purpose, the observed behavior of the generated ions in the presence of various neutral reagents can provide good support for the proposed structures. For example, the isomeric allyl, 2-propenyl, 1-propenyl, and cyclopropyl anions generated in the gas phase by CID of the corresponding carboxylate anions have been detected with a Fourier transform mass spectrometer (FTMS).[4] The observed CS_2 or N_2O reaction products in the aforementioned study[4] serve to differentiate the allyl anion from the vinyl and cyclopropyl anions.

In this paper, we report for the first time evidence for the coexistence of two gas-phase structures of CHS_2^- produced in a chemical ionization source and their regioselective reactions with CS_2 (**1**), which has proven to be a useful structure-probing neutral reagent for our study. Ab initio calculations, described for each CHS_2^- ion structure and its ion−molecule reaction with CS_2, provide additional insight into the two proposed structures. Density functional theory (DFT) calculations (using the hybrid functional B3LYP) were also performed to assess the ability of this method to describe such systems.

Experimental Section

Gas-Phase Anion Chemistry. Carbon disulfide was ACS reagent grade from Aldrich Chemie and was used without further purification. The 75%/25% CH_4/N_2O gas mixture was prepared by Air Liquide using N45 grade CH_4 and N48 grade N_2O.

A Finnigan MAT TSQ70 mass spectrometer was operated under chemical ionization conditions. The ionization gas was a mixture of 75%/25% CH_4/N_2O at a pressure of 8 Torr (uncorrected gauge reading). Source operating conditions were: electron energy, 100 eV; emission current, 50 mA; repeller voltage, 0 V. The CS_2 reagent was intoduced through the gas chromatograph (GC) inlet in the chemical ionization (CI) high-pressure source. Target CS_2 was introduced into the collision cell at a pressure of 3 mTorr (uncorrected gauge reading).

Computational Method. All theoretical structures were optimized by the gradient techniques implemented in GAUSSIAN 94,[5] with HF, MP2(fc), and Becke's three-parameter hybrid function incorporating the Lee−Yang−Paar correlation function (B3LYP).[6] The 6-31++G(d,p) basis set was used for geometry optimizations. The character of the stationary points and the zero-point energy corrections were obtained from analytical frequency calculations.

At geometries optimized using the MP2/6-31++G(d,p) wave function, the energies were recalculated at the QCISD(T)/6-31++G(d,p) level for the larger system (CS_2H^-/CS_2) and at a slightly modified G2 level[7] for the H^-/CS_2 system. The modifications with respect to the standard G2 approach were the following: (i) calculation of the vibrational frequencies at the B3LYP/6-31++G(d,p) level; (ii) the base energy level (step 3) and ΔE^{QC1} (step 6) are calculated using the 6-311++G(d,p) basis set and then step 4 (calculation of ΔE^+) was eliminated;

S1089-5639(97)03089-2 CCC: $15.00
Published on Web 05/02/1998

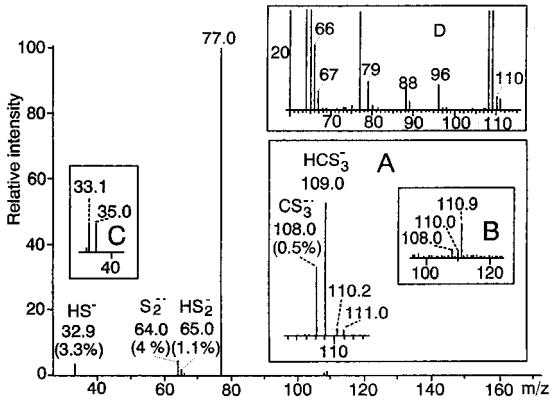

Figure 1. Reactive collision spectrum of the selected $HC^{32}S_2^-$ ions (*m*/*z* 77) with CS2 as collisional reagent in the collision cell at 10 eV offset voltage and at $P_{CS2} = 3$ mTorr, uncorrected gauge reading). Box A displays the region 105th−115th amplified 100 times accompanied in the same window (box B) by a similar region displayed in spectrum recorded by reactions with the labelled $HC^{32}S^{34}S^-$ ions as selected main beam (*m*/*z* 79 instead of *m*/*z* 77). Box C displays the produced ions in the 30−40th region from the latter-selected labeled ion. Box D display the region 60^{th}−120^{th} with 0.2% relative intensity full scale from reaction with the unlabelled selected *m*/*z* 77 ions.

and (iii) in step 8 (calculation of Δ^{G2}), a diffuse function was also added to the hydrogen atom.

In some cases in which bond breaking occurs, the stability of the restricted wave function has been tested; no open shell contribution to the wave function was found. All partial charges were based on the natural population analysis (NPA)[8] of the Hartree−Fock electron density. Natural bond orbital (NBO)[8] calculations have also been performed to analyze some delocalization interactions.

Results

Mass Spectrum Experiments. *Formation of the CHS_2^- Ions.* The negative ion chemical ionization (NICI) of CS_2 with CH_4/N_2O results mainly in the formation of ions *m*/*z* 76, $CS_2^{\bullet -}$, by an electron-transfer process, and ions *m*/*z* 77, CHS_2^-, arising from a hydride attachment. The intensity of the *m*/*z* 77 ions is 27% of the base peak at *m*/*z* 76. The *m*/*z* 77 ion is mainly $(CHS_2)^-$, contaminated by the $^{13}CS_2^{\bullet -}$ (1.1%/0.27 = 4.1%) and $C^{33}S^{32}S^{\bullet -}$ (0.75% x 2/0.27 = 5.6%) natural isotopic ions. Thus, a priori, 9.7% of the *m*/*z* 77 peak intensity results from isotopes of $CS_2^{\bullet -}$, with the remainder (>90%) attributable to the $(CHS_2)^-$ ions. All the observed ions should be relatively stable species because they were internally stabilized by a large number of low energy collisions achieved in the pressure source.

Ion−Molecule Reaction between Anions CHS_2^- and CS_2. To study various ion−molecule reaction channels induced by the selected CHS_2^- reagent ions, a tandem mass spectrometer as triple quadrupole instrument was used. These experiments were performed by selected transmission of the ions (*m*/*z* 77) CHS_2^- from the first quadrupole (by maintaining constant the RF and DC voltages fixed on *m*/*z* 77). These ions transferred in the second RF-only quadrupole (used as collision cell) at low offset voltage values (i.e., laboratory energy as $E_{lab} = 10$ eV) were submitted to multiple collision processes with CS_2, yielding very likely vibrational energy relaxation concomitant to reactive collision as well as CID in lower contribution. The product ions were analyzed by scanning the RF and DC voltages of the third quadrupole. The reaction of $(CHS_2)^-$ yields several ions, which are indicated in Figure 1. The ions at *m*/*z* 109 (1%) and *m*/*z* 108 (0.5%) correspond, respectively, to elemental formulas HCS_3^- and $CS_3^{\bullet -}$ (Figure 1, box A). The peak at

SCHEME 1

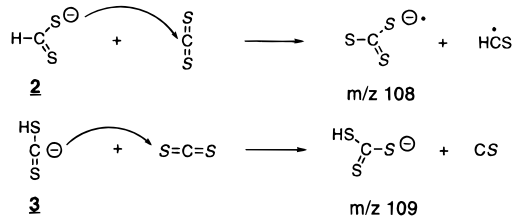

m/*z* 109 shifts to *m*/*z* 111 in the reaction of $CH^{34}S^{32}S^-$ (*m*/*z* 79) with CS_2, reflecting the incorporation into the adduct ion of the two sulfur atoms of the starting anion, whereas the peak at *m*/*z* 108 is partially shifted to *m*/*z* 108, *m*/*z* 110 in a 50/50 ratio, reflecting the fact that only one sulfur atom from the reagent anion is incorporated in these ions (Figure 1, box B). Ions at *m*/*z* 65 (1.1%) partially shifted at *m*/*z* 67 (resulting from a fragmentation of $[CHS_2 + CS_2]^-$ adducts according to an undetermined mechanism) and not shifted at *m*/*z* 64 (4%)[9] are also present (Figure 1, box D), as are the partially shifted ions at *m*/*z* 33 (3.3%) (Figure 1, box C). Elemental formulae for these ions are, unambiguously, HS_2^-, $S_2^{\bullet -}$, and HS^-, respectively.

Discussion

Examples of hydride transfer reactions of negative ions can be found in the literature;[10] for example, it has been shown that it is possible to reduce in the gas-phase some aldehydes lacking α-hydrogen atoms with methoxide ion.[11] Gas-phase transfer of hydride from various anions to CS_2 yielding CHS_2^- ions has been observed.[12] In all these studies, the H^- is implicitly reported to bond to form the dithioformate $H-CS_2^-$ anion **2**. However, a second reasonable possibility in which an H−S bond is formed cannot be ignored. To our knowledge, there are no reports of gas-phase fragmentation or ion−molecule reactions occurring with the reagent CHS_2^- ions, which could afford further insight into the structure of these anions. The results of the reactions of the CHS_2^- ion with the neutral reagent we have used are given in Figure 1. The structures of the product ions proposed in Scheme 1 have been deduced from their *m*/*z* ratio and from the ^{34}S isotopic studies (the origins of the different sulfur atoms are indicated by Roman and italic S atom).

Such structures imply the existence of two possible isomeric forms for CHS_2^- that react regioselectively with CS_2: one results from the addition of H^- to the carbon atom (thioformate ion, **2**), and the other from the addition of H^- to one of the sulfur atoms (thiohydroxythiocarbonyl ion, **3**). The observed behavior of each of these anions in the presence of carbon disulfide provides evidence for the structures depicted in Scheme 1: (i) The thioformate anion reacts by nucleophilic attack on the carbon of CS_2 (carbophilic attack), followed by fragmentation to yield the $CS_3^{\bullet -}$ ion (*m*/*z* 108). (ii) The thiohydroxythiocarbonyl ion reacts by nucleophilic attack on one of the sulfur atoms of CS_2 (thiophilic attack), inducing the characteristic loss of the CS neutral[12] to yield the HCS_3^- ion (*m*/*z* 109).

Experimental evidence for the formation of the thiohydroxythiocarbonyl species is provided by the presence in the CID spectrum of a peak at *m*/*z* 33 coming from the $HS-C^-{=}S$ ions (Figure 1, box C). This peak is partially shifted to *m*/*z* 33 and *m*/*z* 35 when *m*/*z* 79 ($H^{34}SC^{32}S^-$) is allowed to react with CS_2. This *m*/*z* 33 ion is also present in the daughter spectrum of CHS_2^- when xenon was used as the collision gas producing CID. It is not possible to quantify from these results the contribution of both the $HSCS^-$ and HCS_2^- isomeric form

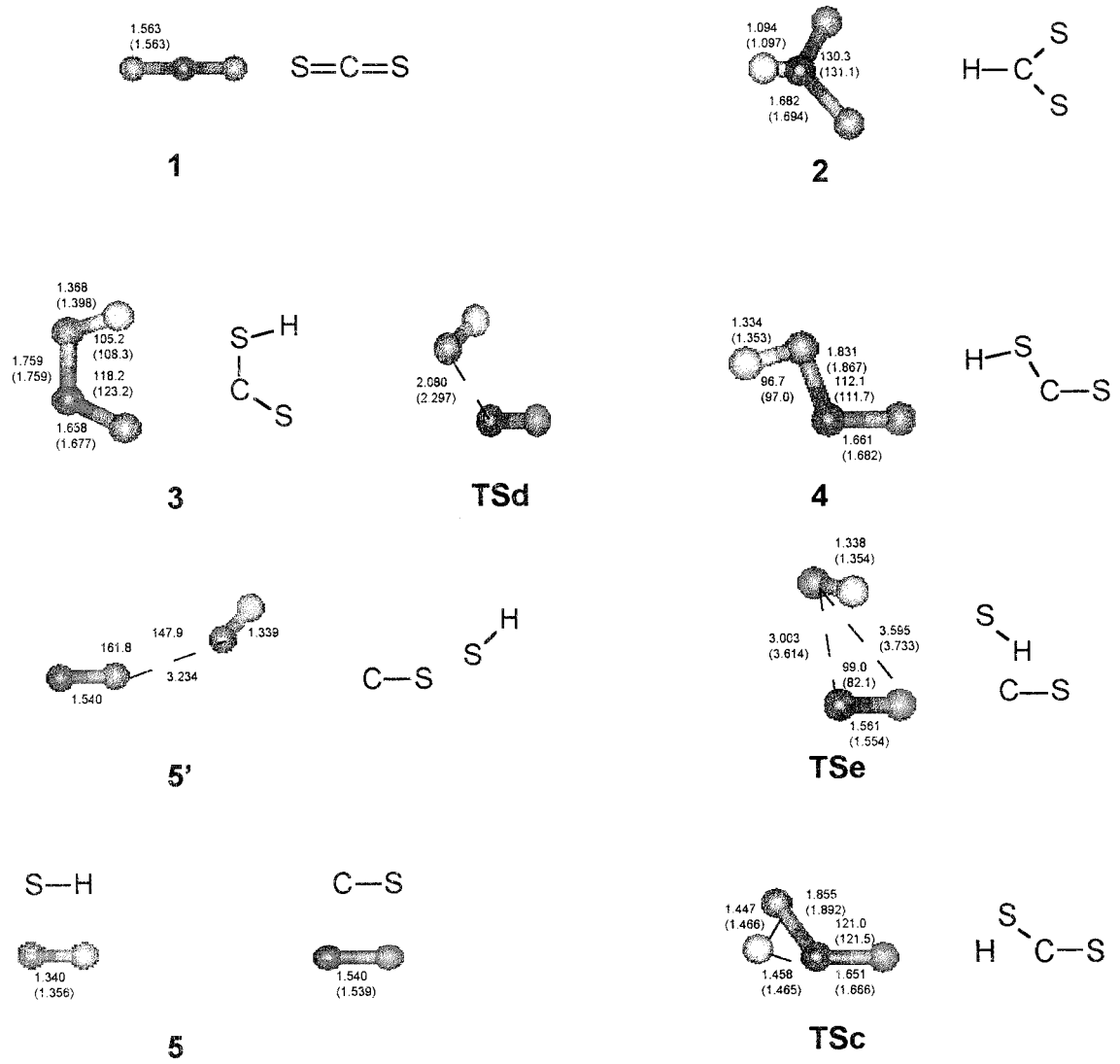

Figure 2. Geometric parameters of various structures relevant to the CS_2/H^- system; selected bond distances (in Å) and bond angles (in degrees) at the MP2(fc)/6-31++G(d,p) and B3LYP/6-31++G(d,p) (in parentheses) levels are shown in the figure.

because relative abundance of the HCS_3^- an $CS_3^{\bullet -}$ ions cannot be connected.

Finally, because Lee and Bierbaum[13] have shown in a series of flow-tube experiments of the reactions of $^{34}S^-$ with the CS_2, COS, and H_2S neutral that rate constants and reaction channels can vary depending on the collision energy (in the range of 1 eV) and have demonstrated that ion−molecule reactions between S^- and CS_2 leading to sulfur exchange were characterized by negative energy dependence, we verified in our study (the collision offset voltage is incremented between each scan from 0 to 20 V by 0.2 V, collision gas is only CS_2) that that was not the case. Furthermore, under our experimental conditions a large kinetic energy distribution is likely carried out at the CI source exit lens by the selected anions, which explains the production of both the reactive and dissociative collisions despite the low internal energy of the selected main ion beam. It is interesting to note that the reactions of **2** and **3** with CS_2 are extremely slow, whereas the charge exchange reaction between $CS_2^{\bullet -}$ and CS_2 is complete under the same experimental condition (as in footnote 10). This result may be surprising because the activation energies are only 1.5 and 0 kcal/mol for **2** and **3** with CS_2, respectively.

Now, the mass spectrometry results just presented and their interpretation raise several questions: (i) Do the thiohydroxythiocarbonyl carbanion and the thioformate anion interconvert in the gas phase? (ii) Is a hydride transfer from the thiohydroxythiocarbonyl carbanion HS−C$^-$=S to the carbon atom of CS_2 to give H−CS_2^- possible? (iii) Can the different behavior of the two CHS_2^- isomers toward CS_2 be rationalized?

We have carried out ab initio studies for the reaction of H^- with CS_2 and for the reactions of the two CHS_2^- isomeric species with CS_2 to seek answers to these questions.

Theoretical Studies. *Addition of H^- to CS_2.* The stationary points located on the CS_2/H^- potential energy surface are shown in Figure 2 and their relative energies are given in Table 1. The ZPVE, computed from the unscaled B3LYP vibrational frequencies, have been included in Table 1. Finally, the energetic profile of the reactions depicted in Scheme 2 is illustrated in Figure 3.

Two entrance channels have been found. The first corresponds to a C_{2v} approach of the hydride ion and leads to H−CS_2^- **2** (step a of Scheme 2). In the second, the H^- approach occurs initially along the C−S bond axis and gives syn (HS−C=S)$^-$ **3** (step b of Scheme 2). At the B3LYP and MP2 levels, there is no barrier to the formation of **2** and **3**.[14] It is noteworthy that the behavior of H^- toward CO_2 is different in that $HOCO^-$ does not form directly from H^- and CO_2,[15] presumably due to the high electronegativity of the oxygen atom. Step a is strongly exothermic, the B3LYP reaction energy (−78.7 kcal/mol) being close to that of the G2 (−80.0 kcal/

TABLE 1: Relative Energies[a] (kcal/mol) and Zero-Point Vibrational Energies (ZPVE, in kcal/mol) of the Structures Depicted in Figure 2

structure	HF[b]	B3LYP[b]	MP2[b]	G2[c]	ZPVE[d]
2	−85.4	−78.7	−75.9	−80.0	10.4
3	−39.7	−33.2	−27.1	−38.4	7.5
4	−38.3	−31.0	−25.4	−36.2	7.9
5	−29.2	−34.1	−11.5	−20.9	5.6[e]
complex	—	—	−22.6	−28.7	6.4[f]
TSc	2.5	−5.4	0.3	−9.2	5.5
TSd	−25.1	−21.4	−14.6	−31.3	6.6
TSe	−27.0	−15.4	−12.2	−20.6	6.1

[a] All energies relative to $CS_2 + H^-$; total energies (in a.u) of this system are: −832.88521 (HF), −834.49184 (B3LYP), −833.26898 (MP2), and −833.54014 (G2) for CS_2; for H^-, the corresponding values are −0.48707 (HF), −0.53432 (B3LYP), −0.50363 (MP2), and −0.52384 (G2); ZPVE (CS_2) = 4.3 kcal/mol. [b] With 6-31++G(d,p) basis set. [c] Without ZPVE correction. [d] Calculated from the B3LYP/6-31++G(d,p) unscaled frequencies. [e] ZPVE (CS) = 1.9 kcal/mol; ZPVE (SH^-) = 3.7 kcal/mol. [f] Calculated at the MP2/6-31++G(d,p) level.

SCHEME 2

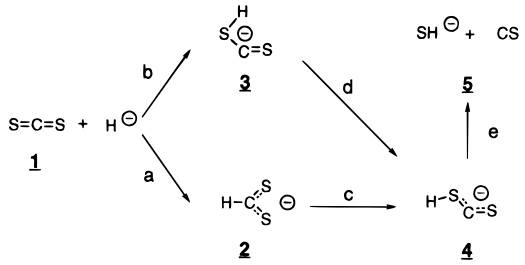

mol). After inclusion of ZPVE corrections, a value of −73.9 kcal/mol is obtained at our best level of theory (see Figure 3). An experimentally derived hydride affinity HA equal to 67.3 kcal/mol has been attributed to CS_2;[16] this value is lower than our calculated HA (73.9 and 72.6 kcal/mol at the G2 and B3LYP levels, respectively). Step b is less exothermic, and the agreement between G2 (−32.6 kcal/mol) and B3LYP (−27.4 kcal/mol) is less satisfactory.

Another interesting feature of the potential energy surface is the absence of a saddle point connecting the anions **2** and **3**. The H migration from the C atom to an S atom occurs only in step c via the **TSc** (Figure 2); this process is strongly endothermic [41.3 kcal/mol (G2); 45.2 kcal/mol (B3LYP)] and proceeds with a very high activation barrier [65.9 kcal/mol (G2); 68.4 kcal/mol (B3LYP)]. These values indicate that the $H-CS_2^- \rightarrow$ anti $(HS-C{=}S)^-$ conversion does not occur under the experimental conditions. At this point, we should briefly discuss the structure and relative stability of the syn and anti anions **3** and **4**. The syn form **3** is the more stable of the two at all levels of calculation by 1.4 to 2.2 kcal/mol. Natural population analysis shows that the charges borne by the H and the terminal S atoms of **3** are, in electron units +0.046 and −0.440, respectively. A weak Coulombic attraction can be expected between these atoms, which stabilizes the syn form **3** to a greater extent. In addition, a close examination of Figure 2 reveals that the S−H bond becomes longer in the syn anion **3**; this observation is consistent with the strongest delocalization interaction in **3** involving the σ^*_{S-H} antibond. Second-order pertubation analysis shows, among all stabilizing orbital interactions, that it is the C lone pair $n_C{}^-\sigma^*_{S-H}$ delocalization that differentiates isomers **3** and **4**.[17] The magnitude of this interaction, calculated by the NBO deletion procedure, is −8.2 kcal/mol in **3** and only −2.5 kcal/mol in **4** because the $n_C{}^-\sigma^*_{S-H}$ overlap is strongest in the former. Thus, we conclude

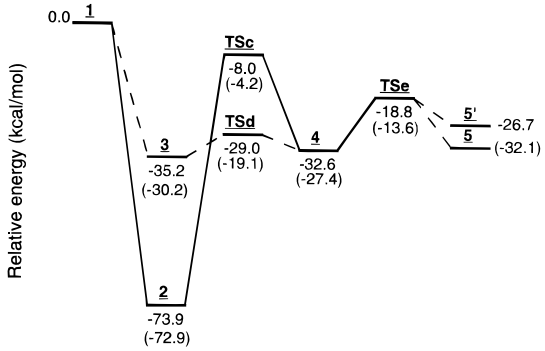

Figure 3. Schematic potential energy diagram showing the reactions given in Scheme 2. Energy values obtained from ZPVE-corrected G2 energies and B3LYP energies (values in parentheses) relative to that of **1** ($CS_2 + H^-$).

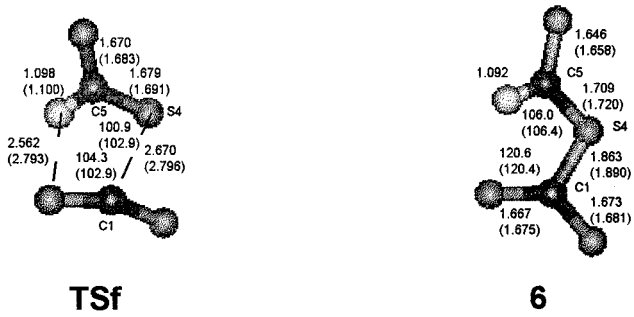

Figure 4. Structures at stationary points for the $HCS_2^- + CS_2$ reaction; bond distances (in Å) and bond angles (in degrees) at the MP2(fc)/6-31++G(d,p) and B3LYP/6-31++G(d,p) (in parentheses) levels.

that the greater stability of the syn $HSCS^-$ anion can be explained, at least in part, by a larger $n_C{}^-\sigma^*_{S-H}$ delocalization energy for this isomer.

Despite our searches, no path corresponding to the **3** → **2** conversion could be found. On the other hand, the interconversion **3** → **4** (step d in Scheme 2) occurs *via* **TSd** (Figure 3). **TSd** is reached for a HSCS dihedral angle of 86° (B3LYP) or 86.5° (MP2; Figure 2); this transition structure is characterized by a large elongation of the C−S(H) bond [0.538 A° (B3LYP) or 0.321 A° (MP2)] with respect to the corresponding bond in **3**. **TSd** lies 10.9 kcal/mol (B3LYP) or 6.2 kcal/mol (G2) above **3**, including ZPVE corrections. The energy difference (including ZPVE corrections) between **TSe** (Figure 3) which connects **4** and **5** (step e in Scheme 2) and **TSd** is 5.5 kcal/mol. (B3LYP) and 10.2 kcal/mol (G2).

In summary, calculations indicate that HCS_2^- and $HSCS^-$ are formed and coexist in the source without structure interconversion, but $HSCS^-$ may decompose to give $CS + SH^-$. Due to the low hydride affinity of the S site in CS_2 (∼35 kcal/mol), the $HSCS^-$ isomer could not have been formed in most previous studies using for examples, CH_3O^-, $HSiO^-$, or $HSiS^-$.

Addition of HCS_2^- to CS_2. The calculations show that HCS_2^- attacks the C atom of CS_2 to give anion **6** via **TSf**; their geometries are given in Figure 4. Barrier height and reaction enthalpy for this elementary step are listed in Table 2. Despite its low exothermicity (−7.5 kcal/mol at our best estimate), HCS_2^- addition proceeds with a very low activation barrier (∼1.5 kcal/mol). One notices that the barrier height is overestimated at the HF level. The features of this potential energy surface differ entirely from those of the reaction of $HCSi^-$ and CS_2 for which a four-membered cycloadduct has been characterized.[18] The key factor determining the direction of the approach of HCS_2^- seems to be the strong stabilizing interaction between one of the lone pairs of S in HCS_2^- and

TABLE 2: Relative Energies[a] (kcal/mol) and Zero-Point Vibrational Energies (ZPVE, in kcal/mol) of the Structures Depicted in Figure 4

structure	HF	B3LYP	MP2	QCISD(T)	ZPVE[b]
TSF	10.8	0.9	0.9	1.3	14.8
6	−4.6	−5.8	−7.4	−8.5	15.7

[a] All energies relative to HCS_2^- + CS_2; in both cases, the 6-31++G(d,p) basis set has been used. [b] Calculated from the unscaled B3LYP frequencies.

SCHEME 3

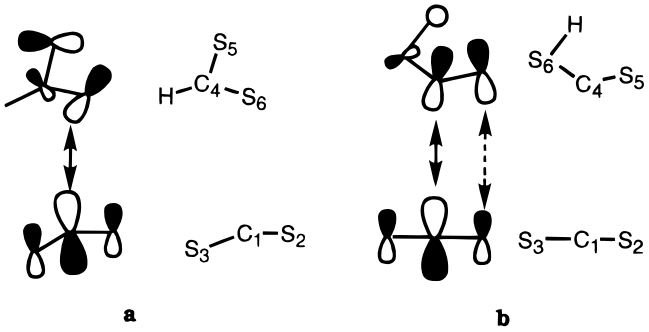

the π^*_{C-S} of CS_2. The magnitude of this interaction, calculated by the NBO deletion procedure, is −44.8 kcal/mol in **TSf**. In terms of molecular orbitals (MO), the corresponding interaction (Scheme 3a) is between the highest occupied b_2 of HCS_2^- and the LUMO (π_u) of CS_2.

Addition of syn HSCS⁻ to CS₂. Structures corresponding to the stationary points of the $HSCS^-$ + CS_2 reaction are shown in Figure 5, and their ZPVE and relative energies are given in Table 3. The calculations indicate that $HSCS^-$ addition occurs with a different regiochemistry than the HCS_2^- addition: in a first step, bond formation between the carbanionic center and an S atom of CS_2 takes place to give intermediate **7**. At the HF level, there is a barrier to the formation of **7**[19] that disappears with inclusion of electron correlation. Intermediate **7** lies above CS_2 + $HSCS^-$ by 14.5 kcal/mol (MP2) and 3 kcal/mol (B3LYP), including ZPVE. This result parallels the structural trend (the C_1-S_3 bond formed in **7** is shorter at the MP2 level; −1.755 versus 1.811 Å). Intermediate **7** dissociates to lead to a loose complex $CS\cdots S_2CSH^-$ **8** *via* **TSg**. At the B3LYP and MP2 levels, weak energy barriers of 0.2 and 1.8 kcal/mol, respectively, including ZPVE, are found for this process. But, this barrier disappears when single-point QCISD(T)/6-31++G(d,p) calculations based on MP2 geometries were performed.

Thus, we can conclude that $HSCS^-$ adds to CS_2 to give CS and S_2CSH^- via a thiophilic approach, without an activation barrier, and with an exothermicity of ∼15.5 kcal/mol. One notices that the B3LYP method underestimates the stability of the three structures.

To understand the preference of $HSCS^-$ toward the S atom of CS_2, the electronic structure of the reactants should be examined. The natural charges of C and S in CS_2 are −0.306 and +0.153 (electron units), respectively, the natural charges borne by C_4, S_5, and S_6 in the $HSCS^-$ ion (see Scheme 3 for numbering) being −0.533, −0.440, and −0.073, respectively. A thiophilic approach of the anion, in which the C_1-S_3 and C_4-S_5 bonds are nearly orthogonal, maximizes the stabilizing electrostatic interactions. In terms of frontier molecular orbital interactions, a carbophilic approach seems a priori to be preferable because the CS_2 LUMO is more concentrated on the C atom. However, the phasing of the appropriate MO (in phase between C_1 and C_4 ↔, out of phase between S_2 and S_5 ⟨···⟩; Scheme 3 b) prevents a strong orbital interaction, which compensates for the expected weaker Coulombic interaction.

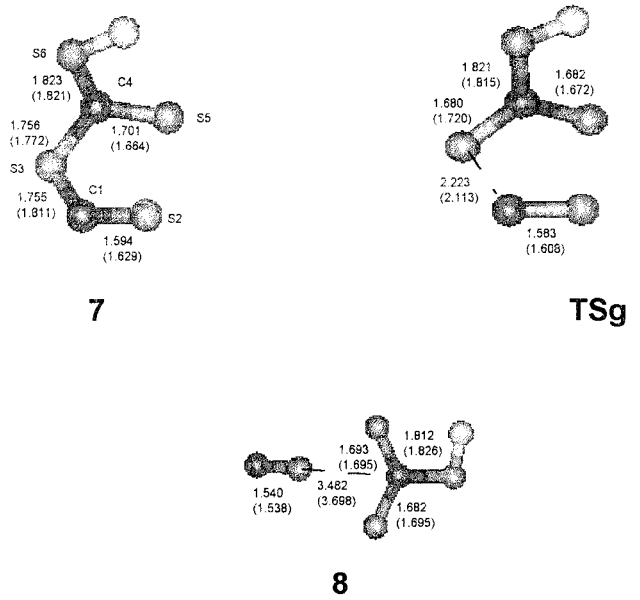

Figure 5. Structures at stationary points for the $HSCS^-$ + CS_2 reaction; bond distances (in Å) at the MP2(fc)/6-31++G(d,p) and B3LYP/6-31++G(d,p) (in parentheses) levels.

TABLE 3: Relative Energies[a] (kcal/mol) and Zero-Point Vibrational Energies (ZPVE, kcal/mol) of the Structures Depicted in Figure 5

structure	HF	B3LYP	MP2	QCISD(T)	ZPVE[b]
7	4.0	−1.4	−12.9	−6.1	13.1
TSg	4.6	−0.8	−10.7	−6.7	12.7
8	−15.8	−6.0	−16.5	−16.1	12.5

[a] All energies relative to $HSCS^-$ + CS_2; in both cases, the 6-31++G(d,p) basis set has been used. [b] Calculated from the unscaled B3LYP frequencies.

Conclusion

Despite the fact that the relative abundances of HCS_3^- and $CS_3^{\bullet-}$ prepared under NICI conditions in a triple quadrupole instrument by anion−molecule reactions induced by CS_2 are only 1% or less of the main beam, it is possible to observe such species. The questions raised from the triple quadrupole experiments have been answered by the ab initio studies in the following way: (i) the relative energies of the CHS_2^- proposed structures have been calculated and indicate that the thioformate and syn thiohydroxythiocarbonyl carbanions are formed without possible interconversion ($HSCS^-$ specifically decomposes into HS^- and CS); (ii) calculations support the postulated mechanistic pathways: the thioformate carbanion reacts with CS_2 at C, whereas the syn thiohydroxythiocarbonyl intermediate reacts at S to ultimately form $HSCS_2^-$ and CS. Finally, the main features of the nucleophilic addition of H^-, HCS_2^-, and $HSCS^-$ to CS_2, given by high-level ab initio calculations, are correctly reproduced at the B3LYP theory level. Thus, this latter method should be applicable with confidence to the study of nucleophilic additions involving larger anions.

Acknowledgment. The authors are indebted to A. Spote and R. Rosenberg for their experimental skills. This work was generously supported by the FNRS (Belgium), the CNRS, and the DRED (France). We are grateful to the CNUSC for the computer facilities. The authors thank the reviewers of this manuscript for helpful comments.

References and Notes

(1) Squires, R. R. *Acc. Chem. Res.* **1992**, *25*, 461.

(2) O'Hair, R. A. J. *Mass Spectrom. Rev.* **1991**, *10*, 133.

(3) For reviews see: (a) Groenewald, G. S.; Gross, M. L. *Ionic Processes in the Gas Phase*; Ferriera, M. A. A., Ed.; D. Reidel: Dordrecht, Holland, 1984; p 244. (b) Holmes, J. L. *Org. Mass Spectrom.* **1985**, *20*, 169.

(4) Froelicher, S. W.; Freiser, B. S.; Squires, R. R. *J. Am. Chem. Soc.* **1986**, *108*, 2855.

(5) Gaussin 94 (Revision B. 3): Frisch, M. J.; Trucks, G. W.; Schlegel, H. B.; Gill, P. M. W.; Johnson, B. G.; Robb, M. A.; Cheeseman, J. R.; Keith, T. A.; Petersson, G. A.; Montgomery, J. A.; Raghavachari, K.; Al-Laham, M. A.; Zakrzewski, V. G.; Ortiz, J. V.; Foresman, J. B.; Cioslowski, J.; Stefanov, B. B.; Nanayakkara, A.; Challacombe, M.; Peng, C. Y.; Ayala, P. Y.; Chen, W.; Wong, M. W.; Andres, J. L.; Replogle, E. S.; Gomperts, R.; Martin, R. L.; Fox, D. J.; Binkley, J. S.; Defrees, D. J.; Baker, J.; Stewart, J. P.; Head-Gordon, M.; Gonzalez, C.; Pople, J. A. Gaussian Inc., Pittsburgh, PA, 1995.

(6) Stevens, P. J.; Devlin, F. J.; Chablowski, C. F.; Frish, M. J. *J. Phys. Chem.* **1994**, *98*, 11623.

(7) Curtiss, L. A.; Raghavachari, K.; Trucks, K.; Pople, J. A. *J. Phys. Chem.* **1991**, *94*, 7221.

(8) For a review, see: Reed, A. E.; Curtis, L. A.; Weinhold, F. *Chem. Rev.* **1988**, *88*, 892.

(9) The recorded reactive collision spectrum of the CS_2 neutral induced by the $CS_2^{\bullet-}$ selected species displays, as expected, only odd-electron sulfide anions at *m*/*z* 32 ($S^{\bullet-}$, 3%), *m*/*z* 64 ($S_2^{\bullet-}$, 31%), *m*/*z* 96 ($S_3^{\bullet-}$, 1%), and polycarbon−sulfide anions at *m*/*z* 88 ($C_2S_2^{\bullet-}$, 2%) and *m*/*z* 152 ($C_4S_4^{\bullet-}$, trace). All these anions as well as $CS_2^{\bullet-}$ are accompanied by species carrying the ^{34}S isotope, indicating that they are produced mainly from the observed dimer (i.e., $[CS_2]_2^{\bullet-}$ and $[CS_2,C^{34}S^{32}S]^{\bullet-}$), rather than by direct CID from the selected $CS_2^{\bullet-}$ anion. Note, in particular, that *m*/*z* 76 is accompanied by *m*/*z* 78 (8%), which indicates that the charge exchange process under multiple collision conditions is very efficient. The presence of isobaric $C^{33}S^{32}S^{\bullet-}$ anions with CHS_2^- in the *m*/*z* 77 signal (5.6%) explains the presence of such fragment species in Figure 1.

(10) (a) Nibbering, N. M. M. *Adv. Phys. Org. Chem.* **1988**, *24*, 36 and references cited therein. (b) Watt, C. I. F. *Adv. Phys. Org. Chem.* **1988**, *24*, 74.

(11) Ingemann, S.; Kleingeld, J. C.; Nibbering, N. M. M. *J. Chem. Soc., Chem. Commun.* **1982**, 1009.

(12) (a) Bierbaum, V. M.; Gravowski, J. J.; DePuy, C. H. *J. Phys. Chem.* **1984**, *88*, 1389. (b) Kass, S. R.; DePuy, C. H. *J. Org. Chem.* **1985**, *50*, 2874. (c) Gronert, S.; O'Hair, R. A. J.; Prodnuk, S.; Sülzle, D.; Damrauer, R.; DePuy, C. H. *J. Am. Chem. Soc.* **1990**, *112*, 997. (d) Kass, S. R.; Guo, H.; Dahlke, G. D. *J. Am. Soc. Mass Spectrom.* **1990**, *1*, 366. (e) Damrauer, R.; Krempp, M.; O'Hair, R. A. J. *J. Am. Chem. Soc.* **1993**, *115*, 1998.

(13) Lee, H. S.; Bierbaum, V. M. *J. Chem. Phys.* **1994**, *101*, 9513.

(14) In contrast, HF calculations predict for step a an energy barrier of 3.0 kcal/mol and a transition structure reached for a C···H distance of 2.0596 Å.

(15) Sheldon, J. C.; Bowie, J. H. *J. Am. Chem. Soc.* **1990**, *112*, 2424.

(16) The hydride affinity scale: Squires, R. R. In Structure/Reactivity and Thermochemistry of Ions; Ausloos, P., Lias, S. G., Eds.; D. Reidel: Dordrecht, 1987; p 373.

(17) The best Lewis structure of **3** resulting from a NBO search is:

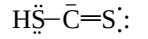

(18) Schmidt, M. W.; Gordon, M. S. *J. Am. Chem. Soc.* **1991**, *113*, 5244.

(19) At the HF/6-31++G(d,p) level, a barrier of 11.1 kcal/mol is obtained for an interfragment S_3-C_4 distance of 2.142 Å (see Scheme 3 for numbering).